Thermographic Phosphors for Gas Turbines: Instrumentation Development and Measurement Uncertainties

Lisbon, Portugal, 2002

J.P.Feist, A.L. Heyes, S.Seefeldt

Department of Mechanical Engineering

Imperial College of Science Technology and Medicine

London, UK

Abstract

Over the past two decades the work on thermographic phosphors was mainly carried out in the US. It is only in recent years that other research groups have explored the field. However, in the future turbine inlet temperatures are likely to increase in order to achieve higher efficiencies introducing greater stress on the components and in particular the turbine blade coatings. Thus there is a general need for advanced temperature detection methods such as thermographic phosphors. When illuminated with UV light they exhibit luminescence, which is temperature dependent by virtue of variations in the relative intensities of distinct emission lines or in the time constant of the exponential decay, which occurs once excitation has ceased. Thermographic phosphors could be employed for temperature detection in the hot section of a gas turbine and this technique promises temperature detection of up to 1400^{o}C with uncertainties better than for other remote standard techniques such as pyrometry.

The paper will address the instrumentation development over recent months and sources of uncertainty when the technique is applied in the field. The paper briefly reviews the application of thermographic phosphors for surface temperature measurements in laboratory combustor of realistic geometry and also includes calculations for the cooling effectiveness.

Uncertainties in the temperature can be caused by the data fitting algorithms, fluctuations of the laser power, changes in oxygen pressure and different gain settings of the detector. When observing the target area through a flame additional radiation can cause a higher noise level than for calibration measurements hence leading to higher uncertainties in temperature. The uncertainties vary with temperature, but usually decrease at higher temperature due to the nature of the calibration data. Highest uncertainties in temperature measurements in the combustor were less than 3.7% for 'cool' areas and less than 1% for 'hot' areas. A simulation of the data detection and processing systems shows the dependencies of the uncertainties on particular input parameters such as noise, observation time, time resolution and digitalization of the signal.

Phosphorescent processes can be pressure sensitive as was demonstrated for so called 'Pressure Sensitive Paints' (PSP) by a variety of research groups. PSPs are widely used for measuring pressure distributions on surfaces. They are sensitive to the partial pressure of oxygen adjacent to the PSP. Thus studies were carried out for two standard thermographic phosphors (Y_2O_3: Eu, YAG: Dy) to simulate pressure changes at different temperatures by changing the oxygen level to investigate the oxygen/pressure sensitivity of these materials. Initial data shows that there is a rather small effect of changing oxygen pressure on the luminescence lifetime decay of the phosphors. For a simulated pressure drop of 0.24bar maximum uncertainties in temperature due to oxygen pressure were estimated to be within 2%.

New instrumentation has been developed and successfully tested for the simultaneous observation of the two temperature modes - lifetime decay and intensity ratio mode - of YAG: Dy. This opens the possibility of crosschecking the temperature during application and extends the dynamic range of the phosphor.

1 Introduction

The quest for better efficiency in gas turbines is inextricably linked to increasing turbine entry temperatures. Stein (1998) stated that a modern stationary gas turbine such as the AS120 from AlliedSignal operates with a pressure ratio of 21:1 and a turbine entry temperature of about 1057°C, but that in the foreseeable future manufacturers will aim for 40:1 and 1400°C for industrial applications.

The extreme temperatures often exceed the mechanical limits of the flow confining materials. In order to guarantee the survival of the turbine parts, mainly within the combustor section and the initial turbine stages, additional thermal protection is needed. This is achieved by the use of ceramic thermal barrier coatings (TBC) and the use of active cooling. Probably the most common method currently employed is film cooling which involves ejecting cool air drawn from the compressor over the surface of components thus creating a protecting film.

The air used for cooling is drawn from the main gas path and thus represents a loss in the overall efficiency of the cycle so that it is therefore important to make the most efficient use of the minimum amount of air. A recent example of research in film cooling includes Schulz (2000) and an early example is that of Goldstein (1971). Detailed experimental work has been mainly focused on rigs of simplified geometry and flow. This work has enabled many critical aspects of film the cooling phenomena to be established since under simplified conditions these can be studied in isolation.

Ultimately however, it will be necessary to carry out investigations at conditions that represent the application as closely as possible. Unfortunately, measuring surface temperature and heat flux under the harsh condition encountered in gas turbines is somewhat problematic. High temperature measurement techniques that have been utilised include thermocouples, Dunker (1992) and Bird, Mutton et al. (1992), thermal paints, Bird, Mutton et al. (1992), and pyrometry, Douglas, Smith et al. (1999) and Alaruri, Bianchini et al. (1997).

Another technique for surface temperature measurement is thermographic phosphor thermometry. Thermographic phosphors have been used in gas turbine research for about twenty years and are reviewed in Allison and Gillies (1997). When the phosphors are illuminated by UV light, they emit phosphorescence at longer wavelengths. Some of the properties, such as the decay lifetime of a transiently excited phosphor, can be used to determine the temperature. This non-intrusive measurement technique overcomes many problems usually connected with high temperature measurements in gas turbines. For example, it is less susceptible to measurement conditions, cleanliness of the optics and background radiation than is pyrometry. There are numerous phosphors available each with a different dynamic range so that they can be matched to a variety of applications including the full range of surface temperatures in current and near future gas turbines. Phosphors can be applied in very thin layers thus yielding the substrates temperature with minimal error. It should be noted however, that the application of reliable thin coatings is difficult with out advanced coating methods such as vapour deposition.

Presently further development of the work carried out at Imperial College London by the authors and reviewed in Feist and Heyes (2001) is underway. The previous work has included the investigation and calibration of a range of phosphors and phosphor response modes. Instrumentation suitable for the application of the technique in a laboratory combustor rig has been developed and a study of the surface temperature distribution and cooling effectiveness in a combustor operating at a scaled take-off condition carried out. Herein we describe the development of improved instrumentation and data processing methods undertaken in the light of this previous experience. In the combustor, measurement uncertainty was observed to increase over that seen in calibration experiments. It was considered possible that oxygen quenching could be an uncalibrated contributory factor in the combustor where the partial pressure varies due to consumption in the combustion reaction. The effect has therefore been studied under calibration conditions by flooding the calibration furnace with controlled amounts of nitrogen. A Monte Carlo simulation of the signal acquisition and processing system has also been conducted with a view to optimising the system. Finally new instrumentation has been developed and tested that will allow simultaneous observation of two phosphor response modes thereby extending the useful dynamic range of those phosphors that exhibit dual response.

2 Instrumentation

In this section various instrumentation setups are described. These include: that used for calibrating the phosphors, the experimental combustion chamber in which wall temperature measurements were taken and the new instrument for simultaneous measurement of the lifetime decay and intensity ratio temperature modes.

2.1 Calibration setup

The setup, originally used by Feist and Heyes (2000), for calibration measurements is shown in figure 1. A sample coated with thermographic phosphor is situated inside a modified furnace. It is illuminated by a UV light from a Nd:YAG laser, which can be tuned to the relevant harmonic wavelengths (266nm or 355nm). A power meter is used to monitor the laser output. The emitted light is captured by a spectrometer and the relevant wavelengths transmitted to a photomultiplier. Both the power meter and photomultiplier data is relayed to a PC for processing.

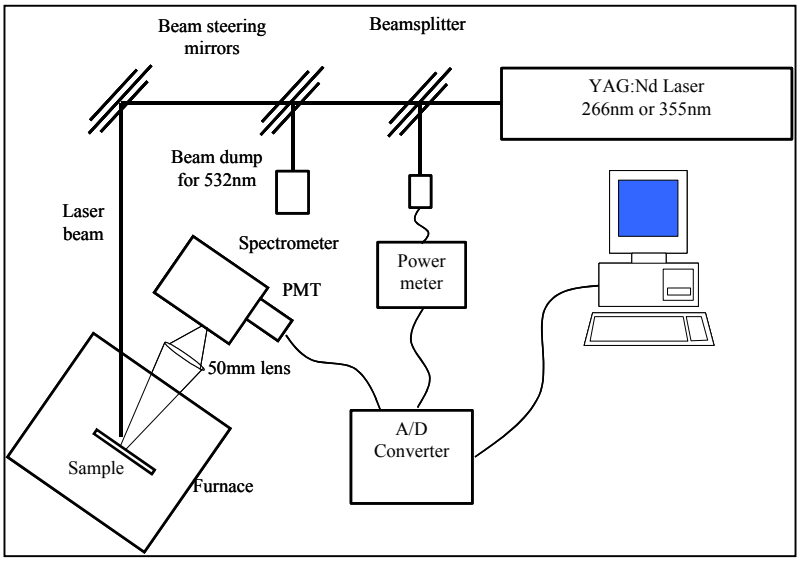

Figure 1: Sketch of phosphor thermometry calibration set.

In the study of the response of thermographic phosphors to oxygen quenching (similar to that known to occur in pressure sensitive paints), the furnace was modified so that oxygen levels could be altered, by the controlled introduction of nitrogen gas. Oxygen levels were measured using a water cooled gas sampling probe connected to an oxygen gas analyzer (ADC7000, Analytical Development Company Ltd.).

2.2 Combustor rig

Surface temperature measurements were made in a laboratory combustion chamber operating at a scaled take off condition and atmospheric pressure. A detailed description of this experiment can be found in Feist and Heyes (2001). The combustor is shown in figure 2 wherein the measurement region is clearly visible.

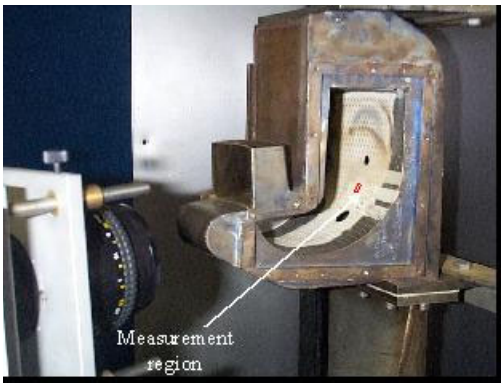

Figure 2: Picture of experimental combustor. Camera lens can be seen on the left. Red square indicates measurement area.

2.3 Instrument for simultaneous lifetime decay and intensity ratio observation

Thermographic phosphors respond to changes in temperature with changes in the decay rate of phosphorescence that occurs once excitation ceases. Certain phosphors, such as YAG:Dy, also respond under continuous or transient excitation with changes in the relative intensity of particular lines in their emission spectra., see Allison and Gillies (1997), Goss, Smith et al. (1989). In the case of YAG:Dy the relevant wavelengths are 455nm and 494nm respectively. The physical process which determines the intensity ratio method is independent of the lifetime decay and is described by Allison and Gillies (1997) and Feist (2001).

An instrument has been designed to simultaneously measure both the intensity ratio and the lifetime decays characteristics of YAG:Dy. This will allow temperature to be determined by two independent methods. A schematic of the instrument is shown in figure 3. Phosphorescence is captured using a camera lens and focused onto a pinhole. Inside the instrument the light is collimated and split into the two relevant wavelengths of 455nm and 494nm using two filters and a dichroic mirror. Two photomultipliers then used to detect the phosphorescence. The instrument has been tested using the calibration set-up shown in figure 1. It was positioned so as to replace the spectrometer with its two photomultipliers connected to two channels of the A/D converter. During calibration experiments the phosphorescence associated with 25 excitation laser pulses was recorded and averaged. Each pulse was recorded with 400 samples at a sampling frequency chosen to cover the majority of the exponential decay. Processing was conducted using a commercial software package. Changes in the gain of the photomultiplier and hence in the recorded intensities were calibrated by using a stable tungsten lamp.

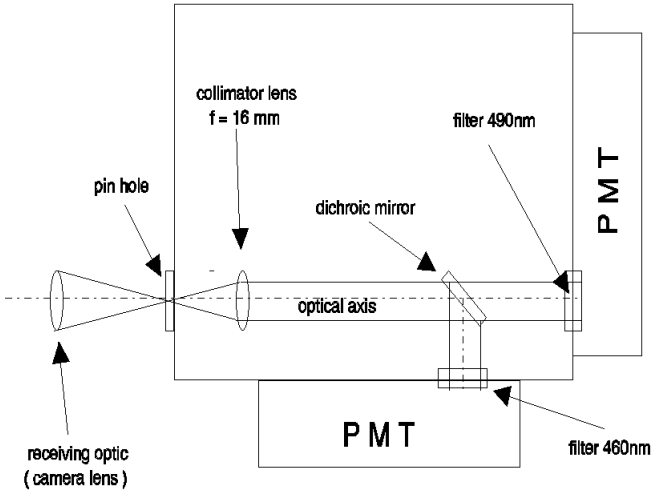

Figure 3: Sketch of instrument used for simultaneous measurement of decay lifetime and intensity ratio.

3 Results

In this section the temperature measurements taken inside the laboratory combustor are briefly reviewed. The investigation of oxygen quenching and the numerical study of uncertainty in the data processing are then presented. Finally, calibration data for the new dual mode detector are discussed.

3.1 Combustor measurements

Figure 4 shows the temperature distribution that was measured over a 8mm by 8mm area within the experimental combustor liner. 128 point measurements were taken over this area. The temperature distribution ranges from 300° to 600°C.

The area considered is subjected to full coverage film cooling. The effects of five film cooling holes can be seen on the temperature map, the three cold spots across the center line and the tips of two further holes near the bottom. The thermographic phosphor was also applied within the depressions at the cooling hole exits so that temperatures could be obtained over the entire area.

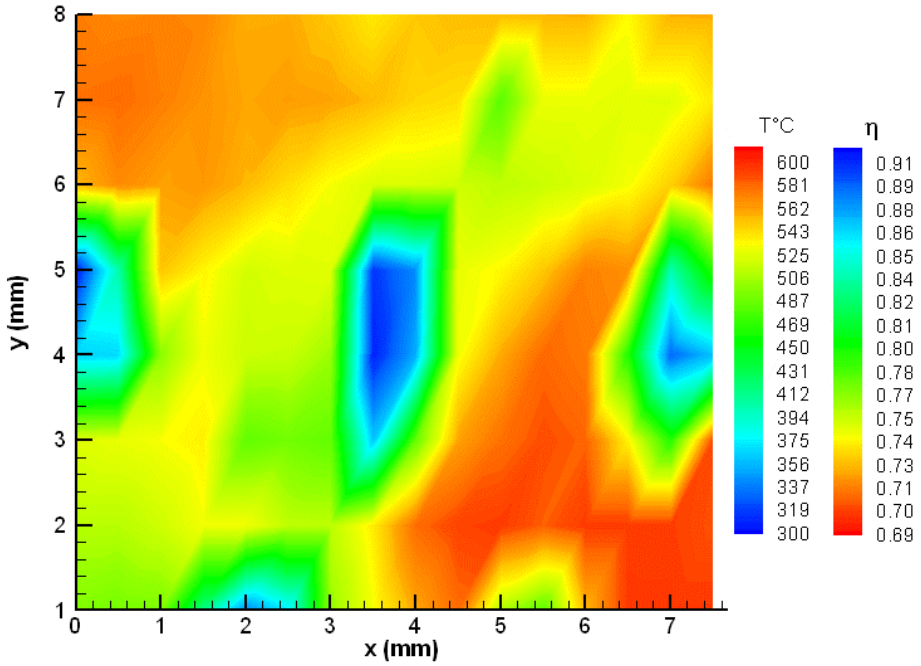

Figure 4: Wall temperature distributions measured over 8mm x 8mm area in an experimental combustor

Temperatures near the cooling holes rise steeply from above 300°C to 500°C. No visible cool streaks appear downstream of the cooling holes. The two hot spots at the top left and bottom right of the measurement region are approximately 550°C and 600°C respectively.

A non-dimensional temperature η is also shown as an indication of cooling effectiveness. This is calculated using (1), where T is the measured temperature T_∞ is the mainstream temperature, which is approximated as the mean exit temperature of the combustor and T_C is the coolant temperature.

$$\eta = \frac{T - T_\infty}{T_C - T_\infty} \tag{1}$$

The mean exit temperature for this combustor was determined by Jelercic (2001) under the same operating conditions as described in Feist and Heyes (2001).

3.2 Sources of uncertainty

3.2.1 Combustor measurements

Uncertainties were estimated for the temperature measurements in the combustion chamber by considering a number of contributory factors. The measurements were corrected for known uncertainties sources and details can be found in Feist (2001). The local temperature uncertainty, ΔT, was calculated using the following equation (2).

$$\Delta T = \nabla(T)\left(\sigma_{laser} + \sigma_{s\tan dard}(x,y)\right) \quad (2)$$

∇(T) represents the gradient of the temperature – decay lifetime relationship. The gradient ∇(T) was determined by the derivative of a fifth order polynomial fit applied to the calibration data. To obtain the uncertainty in temperature the gradient was multiplied by the uncertainties $\sigma_{standard}$ and σ_{laser}. $\sigma_{standard}$ is the local uncertainty in the lifetime decay τ based on five repeated measurements. σ_{laser} is the uncertainty in the laser intensity, which can cause variations in τ at high laser fluxes. Uncontrolled, the laser output energy was observed to fluctuate by as much as ±8%, which would correspond to an uncertainty in the decay time constant of ±7.2μs and serves to confirm the importance of continuous monitoring of the laser energy. Each temperature measurement was derived from the averaged signal from 15 laser pulses. The phosphor used for the measurements was Y_2O_3:Eu.

The gradients in the calibration data ranged from around –2.0°C/μs at 300°C to –0.5°C/μs at 500°C. Highest uncertainties occur where the calibration curve is steepest i.e. in this case at lower temperatures. This is the region that would normally be regarded as being outside the useful dynamic range of the phosphor. However, the temperatures in the combustion chamber extended into this region for the Y_2O_3:Eu phosphor used. Consequently high uncertainty was indicated near the injection holes where the temperatures were lowest. In these regions the highest overall uncertainties, including the effects of laser power fluctuation, were between ±2-3.7%. In higher temperature regions, within the normal dynamic range of the phosphor, a more typical uncertainty was ±0.5%.

3.2.2 Oxygen sensitivity

Thermographic phosphors are similar to pressure sensitive paint (PSP), in that when illuminated with UV light both show luminescence and both enable measurements by means of an exponential decay in luminescence. However, PSP's are sensitive to changes in oxygen levels and also to changes in temperature, while thermographic phosphors are stated as being essentially pressure independent, Allison, Cates et al. (2000). PSP's are mainly used for aerodynamic studies within wind tunnels and turbomachines, such as work by Gouterman (1997) and Engler, Klein et al. (2000). Tianshu, Campbell et al. (1997) review temperature and pressure sensitive paints as well as thermographic phosphors and indicate the similarities of the methods.

Luminescence within the thermographic phosphors is quenched through vibrational effects within the lattice that are temperature dependent. A PSP displays additional changes in the luminescence through oxygen quenching, which is related to the concentration of oxygen diffused into the paint. This in turn can be related to the oxygen partial pressure and thus the overall pressure for a known flow constitution. Since PSP's are also temperature sensitive they must be corrected as shown by Coyle and Gouterman (1999).

Experiments conducted by the authors using thermographic phosphors have been at atmospheric pressure and therefore absolute pressure variations are of secondary concern. However, oxygen partial pressure is certain to fall within combustion chambers due to its consumption in the combustion reaction. Most PSP applications are at low temperatures relative to those of interest herein. Allison, Cates et al. (2000) tested the viability of using thermographic phosphors to correct PSP measurements for temperature variation, the phosphors being shown to be pressure insensitive. However, the experiments were all conducted at temperatures of less than 300°C. Hence, the phosphors used by Allison, Cates et al. (2000) were for low temperature applications and to confirm the findings at higher temperatures the authors have tested Y_2O_3:Eu and YAG:Dy for decay lifetime oxygen dependency.

In the furnace shown in figure 1 the volumetric percentage of oxygen was changed from an atmospheric level of 21% to under 5% by flooding the furnace with nitrogen. This change is equivalent to a pressure drop of 0.24bar in air. Measurements of lifetime decay were taken over a range of temperatures and oxygen

levels. Both temperature and oxygen levels were given sufficient time (15 minutes) to settle between measurements.

Figures 5(a) and (b) display the results of the oxygen sensitivity calibrations for Y_2O_3:Eu and YAG:Dy respectively. Both graphs show the temperature versus decay time in the dynamic temperature range of the phosphors. The individual measurement points show the mean temperatures estimated from the measurements with the maximum and minimum oxygen levels. The error bars show the error in temperature due to the changes in the measured decay time constants. These have been multiplied by a factor of five for illustration purposes.

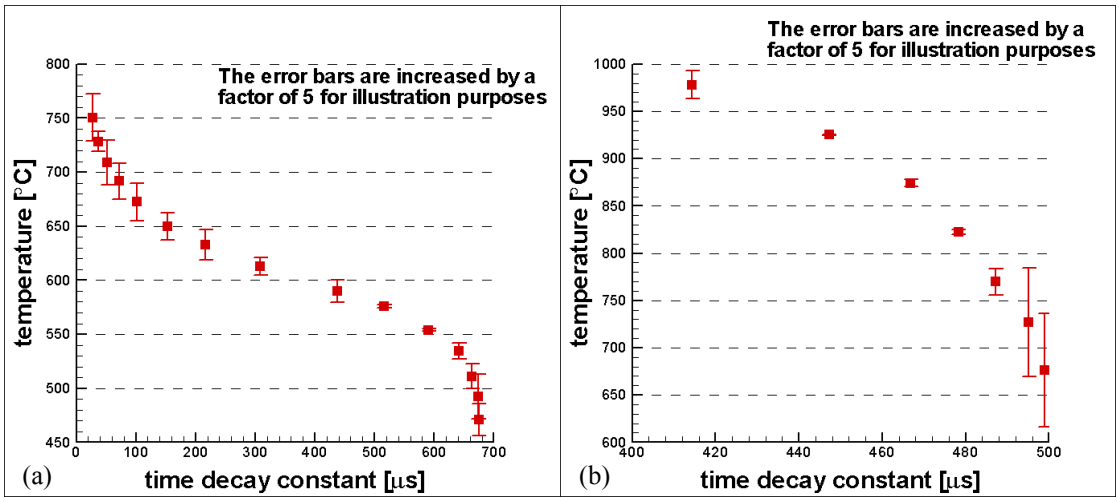

Figure 5: Temperature vs. time decay constant for Y_2O_3:Eu (a)and YAG:Dy (b) from oxygen sensitivity calibration. Error bars show errors in temperature due to changes in oxygen level

Figure 5(a) shows the results for Y_2O_3:Eu over a temperature range from 450°C to 750°C. The largest errors here are within ±4.5°C (0.6%). These can be found at the higher and lower temperatures on the graph. In the region between 500°C and 650°C the errors are below ±3°C. It must be noted that the larger errors occur where the temperature decay lifetime relationship has the least favorable gradient. The actual deviations in τ were larger in the more sensitive area between 500°C and 650°C, but due to the more favorable gradient the errors in temperature are lower.

In figure 5(b) the results for YAG:Dy are plotted over a temperature range of 650°C to 1000°C. The calibration furnace provided the upper temperature limit. As in figure 5(a) the largest errors are located at lower temperatures where the least favorable temperature gradients lie. They peak at ±12°C, which is just over ±1%. The errors in the more temperature sensitive region from 750°C upwards lie within ±3°C.

Note that these errors not only depend on the deviation in the measured lifetime decay, but more so on the local gradient of the calibration curve. Given the large variation on oxygen partial pressure studied combustion driven changes in oxygen levels are not seen as a major source of error during operation of a combustor.

3.2.3 Monte Carlo simulation

During calibration it was recognized that changes in observation length of the exponential decay time can cause changes in the results of the fitting routine. For the lifetime decay method a Levenberg-Marquardt algorithm was utilized to determine the exponential decay of the averaged signal. The quality of this fitting routine depends on a number of parameters including the observation length T. Dowell and Gillies (1991) carried out a Monte Carlo signal simulation to investigate processing procedures for an exponential decay signal. The paper stresses the importance of including an offset C in the exponential decay (3) estimation and stated an optimum normalized observation time $\beta \approx 6$, where $\beta = T/\tau$. The optimum was found by evaluating an error proportionality constant m_N, which was defined by Dowell and Gillies (1991) as in (4), where σ_N is the standard deviation of introduced gaussian noise.

$$I(t) = I_0 e^{-\left(\frac{t}{\tau}\right)} + C \tag{3}$$

$$\frac{\sigma_\tau}{\tau} = m_N \left(\frac{\sigma_N}{I_0} \right) \tag{4}$$

A Monte Carlo simulation similar to the one described by Dowell and Gillies (1991) has been carried out for the specific conditions of the present monitoring system.

The standard and bootstrap Monte Carlo methods were utilized as described by Press, Teukolsky et al. (1994). A schematic illustrating the two methods is shown in figure 6. From an original set of measured data curve parameters (I_o,τ,C) are estimated and used to create simulated sets of data by adding independent, identically and normal distributed white noise. The noise was generated by the Gaussian White Noise routine integrated in the LabVIEW software (Very-Long-Cycle random number). The bootstrap method is distinguished from the standard Monte Carlo method in the way the simulated data in generated. The simulated data is generated by replacing the original data with noisy data. This is illustrated in figure 6 by the dashed line. Usually the bootstrap method is used when not enough information is available to simulate data well. From the simulated data a number of estimates for the given exponential function was obtained. These estimates were statistically analysed.

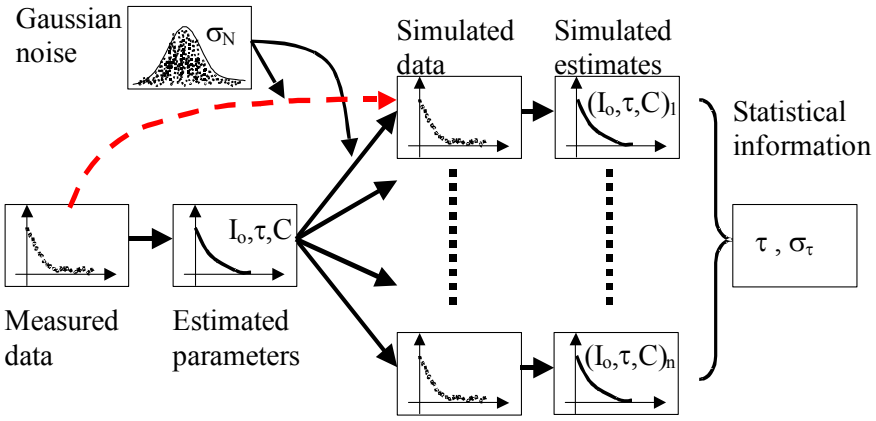

Figure 6: Schematic of the Monte Carlo and Bootstrap methods

The simulations were based on measurements from a Y_2O_3:Eu sample. To achieve a sufficient sample volume 500 simulated data sets were considered for each simulation. The process was carried out for a number of different observation lengths $\beta \approx 1 - 10$. Each simulated data set was composed of 500 sample points, which were equally spaced. The observation time was varied by varying the time step.

Figure 7(a) shows a plot similar to that of Dowell and Gillies (1991) where the error proportionality constant is plotted against β. The standard Monte Carlo simulation produced results similar to Dowell and Gillies (1991) with an optimum observation time at approximately $\beta = 6$. The bootstrap method achieved similar results, but yielded slightly higher errors especially towards higher β's.

(a) (b)

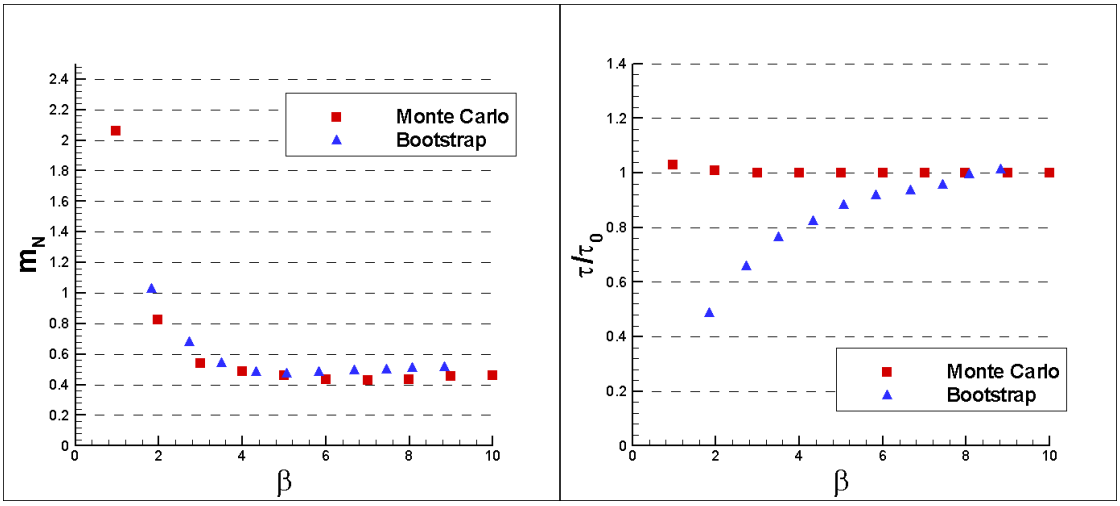

Figure 7: (a) Error proportionality constant plotted against β. (b) Normalized lifetime decay plotted against β. Results are shown from both simulation methods for a Y_2O_3:Eu sample

The situation changes when investigating the normalised decay time τ/τ_0 as shown in figure 7(b). τ is the average estimated decay lifetime and is normalized by the decay lifetime from the original data, τ_0 so that $\tau/\tau_0 = 1$ is the desired result. It can be seen that for the Monte Carlo method this is the case for all but the smallest values of β. However, the results produced by the bootstrap method show an underestimate of τ and only for the highest β values is τ reproduced accurately.

It is hypothesised that the reason for this deviation in decay lifetimes is found in an additional superimposed signal in the early part of the exponential decay, which can be seen in figure 8. Such a signal has been previously reported by Tobin Jr., Beshears et al. (1991) and Feist (2001). The graph shows the actual emission decay signal and the fitted exponential curve. The inlay shows the first 10% of the decay and illustrates the difference between the fitted function and the original data. Shortening the observation time β in figure 8 results in a shortened decay time due to this steeper region of the decay curve.

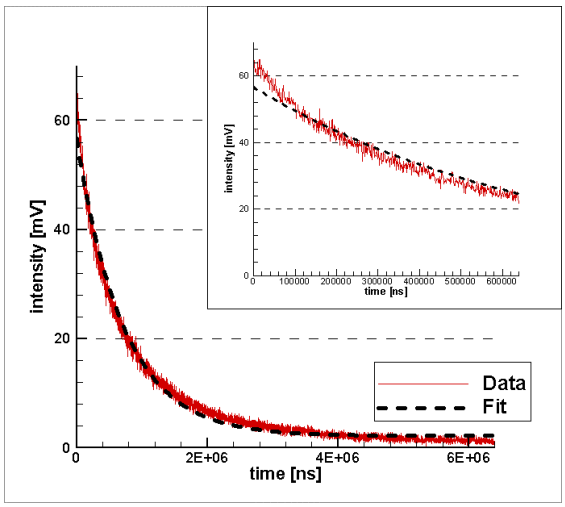

Figure 8: Intensity vs. time plot of Y_2O_3:Eu signal used for simulations. Exponential fit is also shown. Inlay shows first 10% of observation time.

From the present investigations the optimum value of β for precision is around 6 as stated by Dowell and Gillies (1991). However, the bootstrap method shows that for the investigated signal the estimated decay lifetime was not accurate at $\beta \approx 6$. The optimum value of β for accuracy remains to be established but is expected to be in the range 10 to 15.

3.3 Instrument for simultaneous lifetime decay and intensity ratio observation

In figure 9 calibration data for intensity ratio measurements over a range from 300°C to 1130°C are presented. According to the theory described in Goss, Smith et al. (1989) and Feist (2001) the intensity ratio should follow Boltzmann statistics as illustrated by the line in figure 9. The slope of the line is ΔE=1110 cm^{-1} and represents the energy gap between the observed wavelengths expressed in units of the wave vector cm^{-1}. This value is of the right order but various authors have quoted values in the range 1000cm^{-1} to 1653cm^{-1} . The differences in the results are believed to be caused by the crystal field of the YAG host and differences in the optical setup and serve to indicate the importance of system/material calibration.

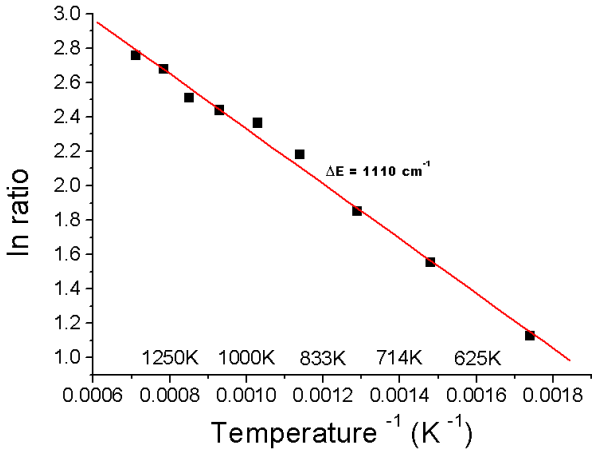

Figure 9: Arrhenius plot of log intensity ratio vs. temperature^{-1} including linear fit for YAG:Dy

Figure 10 shows the lifetime decay constants at wavelengths of 455nm and 490nm plotted against temperature. The graph shows that the most temperature sensitive region of the decay lifetime between 800°C and 1200°C. It can be seen that both emission lines show the same characteristics and therefore represent the same physical mechanism. Similar results were previously obtained with a single photomultiplier.

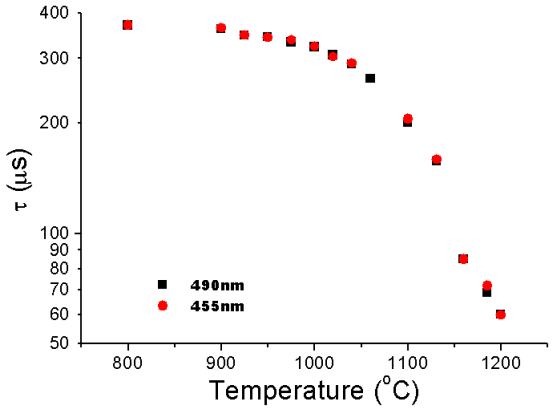

Figure 10: Decay lifetime vs. temperature plot showing decay lifetimes measured at two wavelengths

The results demonstrate the viability of the instrument for simultaneous measurement of decay lifetimes and intensity ratios. This may be particularly useful in circumstances when validation of temperature measurements cannot be achieved by other alternative means. The new instrument also allows the

measurement range of the specific phosphor (YAG: Dy) to be expanded. For lifetime decay measurements it was limited to the range 800°C to 1200°C. Changing from the lifetime decay method to intensity ratio measurement expands the dynamic range down to 300°C.

4 Conclusions

The work presented here is part of the further development of the phosphor thermometry technique for non-intrusive temperature measurements in gas turbines. Various aspects of the development have been outlined.

The uncertainties associated with measurements carried out in an experimental combustor are presented. Uncertainties of ±3.7 % were found where surface temperatures depart from the optimal part of the calibration curve i.e. in low temperature regions at around 300°C. However in higher temperature regions the uncertainty fell to around ±0.5%. Overall the results successfully demonstrate the utility of this technique for real applications in the vicinity of a bright flame.

The decay lifetime sensitivity to oxygen levels of two phosphors, Y_2O_3:Eu and YAG:Dy, was investigated. The maximum error was found to be around 1% and hence is of a similar magnitude to the those within the combustor.

A Monte Carlo simulation of the decay signal was carried out, using two methods of producing simulated data. A minimum in the error proportionality constant was found at normalised observation times $\beta \approx 6$ as previously stated by Dowell and Gillies (1991). However, τ was underestimated at this observation length. Thus for the signals measured in the present investigation a longer observation length is necessary. The measurements presented here were all carried out at a longer observation length.

A dual mode detector was designed and successfully tested for measuring the lifetime decay and the intensity ratio of YAG:Dy at 455nm and 494nm. This can be applied in circumstances when validation of temperature measurements can not be achieved otherwise. The combination of two modes also expands the dynamic range of the specific phosphor in use. The new instrumentation now allows temperature measurements in a range between 300°C to at least 1200°C, (the furnace set the upper limit).

5 Acknowledgements

The authors want to thank the EPSRC for financial support

6 References

Alaruri, S., L. Bianchini, et al. (1997). Effective Spectral Emissivity Measurements of Superalloys and YSZ Thermal Barrier Coating at High Temperatures Using a 1.6μm Single Wavelength Pyrometer. AGARD PEP, Advanced Non-intrusive Instrumentation for Propulsion Engines, Brussels, Belgium.

Allison, S. A. and G. T. Gillies (1997). "Remote Thermometry With Thermographic Phosphors: Instrumentation And Applications." Rev. Sci.Instrum. **7**(68): 2615-2650.

Allison, S. W., M. R. Cates, et al. (2000). "Survey of thermally sensitive phosphors for pressure sensitive paint applications." Instrumentation in the Aerospace Industry : Proceedings of the International Symposium **397**: 29-37.

Bird, C., J. E. Mutton, et al. (1992). Surface Temperature Measurements In Turbines. Symposium on Advanced Non-intrusive Instrumentation for Propulsion Engines, Brussels, AGARD PEP.

Coyle, L. M. and M. Gouterman (1999). "Correcting lifetime measurements for temperature." Sensors and Actuators B **61**: 92-99.

Douglas, J., C. A. Smith, et al. (1999). An Integrated Approach To The Application Of High Bandwidth Optical Pyrometry To Turbine Blade Surface Temperature Mapping. 18th International Congress On Instrumentation In Aerospace Simulation Facilities, Toulouse.

Dowell, L. J. and G. T. Gillies (1991). "Errors Caused By Baseline Off-set And Noise In The Estimation Of Exponential Lifetimes." Review of Scientific Instruments **62**(1): 242-243.

Dunker, R. (1992). Advances In Techniques For Engine Applications, Wiley.

Engler, R. H., C. Klein, et al. (2000). "Pressure sensitive paint systems for pressure distribution measuremtns in wind tunnels and turbomachines." Measurement Science and Technology **11**: 1077-1085.

Feist, J. P. (2001). Development Of Phosphor Thermometry For Gas Turbines. Mechanical Engineering. London, Imperial College.

Feist, J. P. and A. L. Heyes (2000). Development Of The Phosphor Thermometry Technique For The Application In Gas Turbines. 10th International Syposium on Applications of Laser Techniques to Fluid Mechanics, Lisbon, Portugal.

Feist, J. P. and A. L. Heyes (2001). Measurement Of Wall Temperatures In Gas Turbine Combustors Using Thermographic Phosphor Thermometry. International Society for Air Breathing Engines, Bangalore, India.

Goldstein, R. J. (1971). "Film Cooling." Advances in Heat Transfer **7**: 321-379.

Goss, L. P., A. A. Smith, et al. (1989). "Surface Thermometry By Laser-induced Flourescence." Rev. Sci. Instruments **60**(12): 3702-3706.

Gouterman, M. (1997). "Oxygen quenching of luminescence of pressure sensitive paint for wind tunnel research." Journal of Chemical Education **74**(6): 697-702.

Jelercic, D. (2001). Experiments In Annular Combustors. Mechanical Engineering. London, Imperial College**:** 288.

Press, W. H., S. A. Teukolsky, et al. (1994). Numerical Recipes In Fortran - The Art Of Scientific Computing. Cambridge (UK), New York, Melbourne, Cambridge University Press.

Schulz, A. (2000). "Infrared Thermography As Applied To Film Cooling Of Gas Turbine Components." Measurement Science and Technology **11**(7): 948-956.

Stein, H. (1998). "Gas Turbines Will Be Different And Used Differently, In 1998-2007." Turbomachinery International, Handbook **39**(6): 22-23.

Tianshu, L., B. T. Campbell, et al. (1997). "Temperature- and pressure-sensitive luminescent paints in areodynamics." Applied Mechnanics Review **50**(4): 227-246.

Tobin Jr., K. W., D. L. Beshears, et al. (1991). "Fibre-sensor Design For Turbine Engines." SPIE Fibre Optic and Laser Sensors **1584**(IX): 23-31.